ADVANCES IN CEMENT RESEARCH

REPRINT

thomas telford

Advances in Cement Research
Volume 24 Issue 2

Water resistance of composite binders containing phosphogpysum with different pretreatment processes
Ren, Zhu, Liu, Zhu and Yang

Advances in Cement Research, 2012, 24(2), 111–120
http://dx.doi.org/10.1680/adcr.11.00014
Paper 1100014
Received 15/03/2011; revised 02/06/2011; accepted 12/08/2011

ice
Institution of Civil Engineers
publishing

Water resistance of composite binders containing phosphogpysum with different pretreatment processes

Tingyan Ren
MSc student, School of Environmental Science and Engineering, Huazhong University of Science and Technology, Wuhan, China

Jing Zhu
PhD student, School of Environmental Science and Engineering, Huazhong University of Science and Technology, Wuhan, China

Wanchao Liu
PhD student, School of Environmental Science and Engineering, Huazhong University of Science and Technology, Wuhan, China

Xinfeng Zhu
PhD student, School of Environmental Science and Engineering, Huazhong University of Science and Technology, Wuhan, China

Jiakuan Yang
Professor and Vice Dean, School of Environmental Science and Engineering, Huazhong University of Science and Technology, Wuhan, China

The influence of pretreated phosphogypsum on water resistance of composite binders containing phosphogypsum (CBPG) was investigated. Six pretreatment processes in total were conducted on phosphogypsum using autoclaving and calcination. Three parameters of the CBPG mortars were comparatively studied to evaluate their water resistance: the ratio of the compressive strength in the wet-saturated state to that in the dry state (W/D); weight loss after static water attack (WLSW); and weight loss after flowing water attack (WLFW). The crystalline phases could be transformed and the impurities could be effectively purified for original phosphogypsum by the pretreatment process. Therefore, water resistance of the CBPG mortars from pretreated phosphogypsum was improved significantly when compared to that of the mortars from original phosphogypsum. Regarding the weight loss and strength after static or flowing water attacks, WLSW and WLFW could effectively evaluate the water resistance of CBPG mortars, when compared with traditional evaluation by W/D.

Introduction

Phosphogypsum (PG) is a by-product from processing phosphate ore into fertiliser with sulfuric acid. Up to 280 million tonnes of PG are generated annually worldwide (Yang *et al.*, 2009a). In China, approximately 40 million tonnes are produced annually, and only 10% of this is being reused (Huang and Lin, 2010). PG typically contains dihydrated gypsum (>80 wt%) and some impurities including phosphate, quartz, fluorides, organic matter, alkalis, radionuclides and heavy metals (Tayibi *et al.*, 2009). All of these impurities add up to a negative environmental impact and many restrictions on PG applications. A limit of ^{226}Ra in PG set by the Environmental Protection Agency (EPA) is 370 Bq/kg (10 pCi/g). The international limit prescribed by the European Atomic Energy Community (EURATOM) is 500 Bq/kg (13·5 pCi/g) (Değirmenci, 2008). The contents of radioactive elements of PG vary across a wide range, depending on the composition of phosphate rock.

The phosphate and fluorides of PG have adverse effects on setting and hardening of binders (Kitchen and Skinner, 1971; Singh, 2003). Therefore, pretreatment processes are widely used to improve the properties of PG. Potgieter and Howell-Potgieter (2001) and Potgieter *et al.* (2003) studied various physical and chemical treatments to make PG suitable as a set retarder for cement. They also investigated a combined treatment of wet milling of PG with lime slurry and recommended the treatment for full-scale plant applications. Singh *et al.* (1996) conducted a purification process for PG by wet sieving with a 300 μm sieve and a hydrocyclone. Based on the results, a pilot plant with a capacity of 1 tonne per shift was proposed. Singh (2002) also studied treatment of PG with citric acid solutions. The purified PG could then be used to manufacture cement and gypsum plaster. Kovler and Somin (2004) suggested a new technology of topochemical extraction of radioactive salts, phosphates and other impurities from contaminated PG.

In addition to being a retarder in cement production, PG has also been used to produce building materials by mixing with other industrial wastes, such as furnace slag, fly ash and lime. Shen *et al.* (2009) prepared a new type of steel slag–fly ash–PG solidified material as road base material. The strength of the solidified material could meet the Chinese criteria of semi-rigid road base material. Kumar (2003) evaluated the use of fly ash–lime–PG hollow blocks for walls and partitions. Yang *et al.*

(2008) investigated the effect of calcined PG on the strength of fly ash–lime binders. The results showed that the strength of the binder that contained 10% calcined PG increased significantly when compared to the binder with original PG (i.e. without calcination). Kuryatnyk *et al.* (2008) showed that PG could represent an interesting resource for the development of low-cost housing materials. A water-resistant binder was obtained by mixing 70% PG with 30% calcium sulfoaluminate clinker. Garg and Singh (1996) and Singh *et al.* (1990) studied the durability of a PG–lime–fly ash/granulated slag binder by evaluating its performance in water and accelerated aging (i.e. alternate wetting–drying cycles, heating–cooling cycles under temperatures from 27 to 60°C). Yang *et al.* (2009b) investigated the preparation methods for brick with PG and the performance of the brick. The results showed that the strength and durability of the autoclaved bricks made from autoclaved PG were improved.

Although some researchers have reported that PG could be used for preparation of binder/brick and have evaluated the performance of the prepared binder/brick, there are numerous challenges in the application of PG for construction materials, namely cost, radioactivity, public acceptance and water resistance. Among these challenges, water resistance is considered one of the most important properties of gypsum-containing building materials in a humid environment (Bentur *et al.*, 1994; Kovler, 1998). The ratio of the compressive strength in the wet-saturated state to that in the dry state (W/D) is usually used to evaluate the water resistance of a cementitious binder cured for 28 days. However, studies on how to evaluate weight loss and strength after static water attack and flowing water attack are very scarce in the technical literature. In the present study, two parameters for evaluation under static water or flowing water attack environments were used to assess the influence of pretreated PG on water resistance of composite binders containing PG (CBPG), compared with the traditional parameter used for evaluation, W/D.

Experimental work

Raw materials

Phosphogypsum raw materials used in this study were obtained from production of phosphoric acid in a chemical factory in Xiangfan City, Hubei Province, China. The raw PG had water content of 22·50% (by weight) and $CaSO_4{\cdot}2H_2O$ content of 87·13% (by weight) on a dry basis. The radioactivity analyses of PG were carried out by the Supervision and Inspection Bureau of Building Product Quality in Wuhan. The results were ^{226}Ra of 34·50 Bq/kg, ^{232}Th of 0·42 Bq/kg and ^{40}K of 209·44 Bq/kg. The level of radioactivity is much lower than the limit of the Chinese standard (GB/T 6566–2001), so the PG samples can be used for production of construction materials.

Fly ash was taken from a local coal combustion power plant in China. Both lime and ordinary Portland cement (OPC) were purchased locally in Wuhan City, China. The chemical composition of the main raw materials is presented in Table 1.

Pretreatment processes and test methods for PG

In total, six different processes were applied for pretreatment of PG, and the corresponding PG sample designations are listed in Table 2. The original PG is termed PG-0 here, and was obtained by drying the raw PG in an oven at 40°C. PG-A was autoclaved by placing the raw PG in a closed container with steam under a pressure of 0·12 MPa and temperature of 120°C. PG-400, PG-500, PG-600, PG-700 and PG-800 were obtained by calcining PG-A at 400, 500, 600, 700 and 800°C, respectively for 2 h in a muffle furnace. All the PG samples were milled separately by a planetary ball mill until over 85 wt% of particles were at a size of <80 μm.

The amounts of impurities (mainly phosphate and fluoride) in the original and pretreated PG samples were determined. Phosphate levels of PG (original/pretreated) samples were measured using the quinoline phosphomolybdate gravimetric method following the Chinese standard (GB/T 1871.1–1995). Fluoride was determined in accordance with the Chinese standard (GB/T 1872–1995).

The original PG and pretreated PG samples from the muffle furnace were immediately immersed in ethanol for 24 h to terminate the hydration reaction. Subsequently, these samples were dried in an oven at 40°C. In order to compare with the original PG, the pretreated PG samples were analysed by X-ray diffraction (XRD), scanning electron microscopy (SEM) and energy dispersive spectroscopy (EDS). XRD investigations were carried out with an X'Pert Pro diffractometer (PANalytical BV) using Cu $K\alpha$, operated at 40 kV. The scan speed of this equipment was 0·2785°/s, and the 2θ range was from 5° to 65°. SEM analysis was carried out with a Sirion 200 scanning

Constituents	SiO_2	CaO	SO_3	Al_2O_3	Fe_2O_3	MgO	P_2O_5	$K_2O + Na_2O$	F^-	LOI
Original PG	7·07	28·58	39·47	2·89	0·43	0·62	2·35	0·12	0·34	19·08
Fly ash	52·50	5·68	0·50	26·28	3·60	—	—	—	—	2·20
Lime	6·73	60·11	—	—	—	1·50	—	—	—	22·58
OPC	20·57	58·76	2·36	5·39	2·90	3·29	—	0·58	—	4·02

LOI, loss on ignition

Table 1. Chemical composition of raw materials (wt%)

PG sample designation	CBPG mortar designation	CBPG paste designation	Pretreatment process for PG samples
PG-0	M-0	P-0	Original PG
PG-A	M-A	P-A	Autoclaving under a pressure of 0·12 MPa and at 120°C
PG-400	M-400	P-400	Calcining at 400°C of PG-A
PG-500	M-500	P-500	Calcining at 500°C of PG-A
PG-600	M-600	P-600	Calcining at 600°C of PG-A
PG-700	M-700	P-700	Calcining at 700°C of PG-A
PG-800	M-800	P-800	Calcining at 800°C of PG-A

Table 2. Sample designation of PG samples, CBPG mortar and CBPG paste

microscope after the samples had been coated with gold. The microscope was equipped with an energy dispersive X-ray spectrometer (EDAX) to provide elemental analysis of PG samples.

Preparation and testing of CBPG mortars

The CBPGs were prepared by intimately blending 33 wt% PG with 42 wt% fly ash, 20 wt% OPC, 3 wt% lime, and 2 wt% of a suitable chemical activator, followed by grinding in a ball mill. The mass ratio of binder to sand was 1:3, and the mass ratio of binder to water was 2:1. CBPG mortars were cast into a 40 mm × 40 mm × 160 mm steel mould and set for 24 h. After demoulding, these mortars were cured in ambient air at room temperature of 20 ± 5°C for 28 days. Sample designations of CBPG mortars are shown in Table 2. Twelve CBPG mortars for each designation were divided into four groups for performance testing at 28 days of curing.

Three mortars of the first group were dried in an oven at 40 ± 1°C until they reached a constant weight. These dried mortars were used to test the dry strength with the method described in the Chinese standard (GB/T 17671–1999). Three mortars of the second group were immersed in water until saturation, and these mortars were tested for saturated strength. The traditional evaluating parameter (W/D) was used to evaluate the water resistance of CBPG mortars cured for 28 days, which was calculated by

$$1.\quad \mathrm{W/D} = \frac{\text{Compressive strength in wet-saturated state}}{\text{Compressive strength in dry state}}$$

Moreover, weight loss after static water attack (WLSW) and weight loss after flowing water attack (WLFW) were respectively used to evaluate the water resistance of the CBPG mortars cured for 28 days under the static or flowing water attack environment, according to the method suggested by Chen *et al.* (2003).

Three mortars of the third group were dried in the oven at 40 ± 1°C until they reached a constant weight, then immersed in a static water bath for 30 days, and finally dried in the oven at 40 ± 1°C until they reached a constant weight. In the meantime, the dry weights of each mortar before and after immersion were measured, and recorded as W_1 and W_2 respectively. Both weights were used in the calculation of WLSW as follows

$$2.\quad \mathrm{WLSW} = \frac{W_1 - W_2}{W_1}$$

Three mortars of the fourth group were dried in the oven at 40 ± 1°C until they reached a constant weight, then immersed in a flowing water bath with a flow rate of 2800 ml/min for 10 days, and finally dried in an oven at 40 ± 1°C, again until a constant weight was reached. A photograph of the set-up of the flowing water bath for testing WLFW is shown in Figure 1. Meanwhile, the dry weights of each mortar before and after immersion were measured, and recorded as W_1 and W_3 respectively. Both weights were used in the calculation of WLFW as follows

$$3.\quad \mathrm{WLFW} = \frac{W_1 - W_3}{W_1}$$

Figure 1. Photograph of the set-up of the flowing water bath for testing WLFW

Preparation and testing of CBPG pastes

The CBPG pastes were simultaneously prepared and cured in ambient air at room temperature of 20 ± 5°C. Sample designations of CBPG pastes are shown in Table 2. The CBPG pastes were used to test their physical properties with the method described in the Chinese standard (GB/T 1346–2001), including consistency, setting time and soundness.

The CBPG pastes were used to investigate the hydrated phases and morphologies of the hydration products by XRD and SEM. Typical CBPG pastes (P-0 and P-700) were crushed and ground after 7 and 28 days of curing. The samples were immersed and saturated in ethanol for 24 h, then dried at 40°C until they reached a constant weight. The hydration products of CBPG were analysed by XRD (X'Pert Pro), and morphologies of hydration products were investigated by SEM (Sirion 200) after the samples had been coated with gold.

Results and discussion

Comparison of crystalline phase and morphology between original and pretreated PG

The XRD patterns of samples PG-0 and PG-A are shown in Figure 2, and those of samples PG-400, PG-500, PG-600, PG-700 and PG-800 are shown in Figure 3. The XRD patterns showed that the major crystalline phase transformed in these pretreated PG samples, when compared with the original PG sample (PG-0). In sample PG-0, dihydrate ($CaSO_4{\cdot}2H_2O$) is the major crystal. Sample P-A has the main crystal of hemihydrate ($CaSO_4{\cdot}0{\cdot}5H_2O$) with a trace of untransformed dihydrate. Anhydrite ($CaSO_4$) is the main crystal with few hemihydrates in samples PG-400, PG-500 and PG-600, which were made from sample P-A after being calcined at 400–600°C. As the calcination temperature increased to 700°C, all of the gypsum phases were transformed into anhydrite (samples PG-700 and PG-800). Quartz phase (SiO_2) exists in all types of PG samples as a common inert impurity.

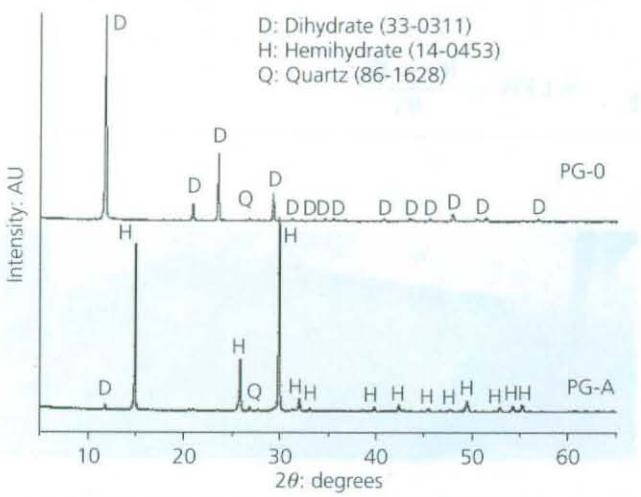

Figure 2. XRD patterns of PG-0 and PG-A

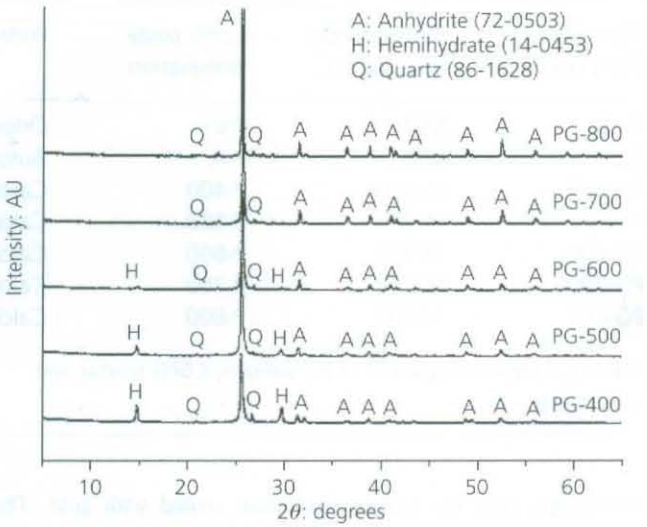

Figure 3. XRD patterns of PG calcined at different temperatures (PG-400, PG-500, PG-600, PG-700 and PG-800)

The SEM/EDS images of the original PG samples are shown in Figure 4. Original PG particles were irregular agglomerates and rhombic crystals, and a large number of granular and flocculent aggregates were attached to the surface of the PG crystal, as shown in Figures 4(a) and 4(b). The chemical element characteristics of the attached matter were investigated with EDS. The smooth surface and attached matter of rhombic crystal were selected as the probe points, respectively, as shown in Figure 4(b). It can be seen that the rhombic crystals are mainly composed of gypsum elements calcium (Ca), sulfur (S) and oxygen (O) (shown in Figure 4(c)), and the attached matter contains many other elements, including phosphorus (P), fluorine (F), silicon (Si), magnesium (Mg) and aluminium (Al) (shown in Figure 4(d)). This implies that impurities were mainly attached on the surface of the PG crystal.

Morphologies of representative pretreated samples of PG-A and PG-700 are shown in Figures 5(a) and 5(b) respectively, and these are significantly different from the morphologies of the original PG shown in Figure 4. The morphology of P-A appears as a rectangular crystalline shape with a smooth surface, which is a typical morphology of α-$CaSO_4{\cdot}0{\cdot}5H_2O$. The morphology of P-700 appears as a rectangular crystalline shape with a coarse surface, which is characteristic of the anhydrite that formed as a result of calcined products from hemihydrate.

Impurities of pretreated PG

The impurities, especially water-soluble phosphorus pentoxide (P_2O_5) and water-soluble fluoride, play important roles in the final PG products. They significantly influence the setting time and strength of PG building materials (Singh, 2003). Therefore, the impurity contents of original PG and pretreated PG samples were quantitatively determined. The measured results of total phosphorus pentoxide, total fluoride, water-soluble phosphorus

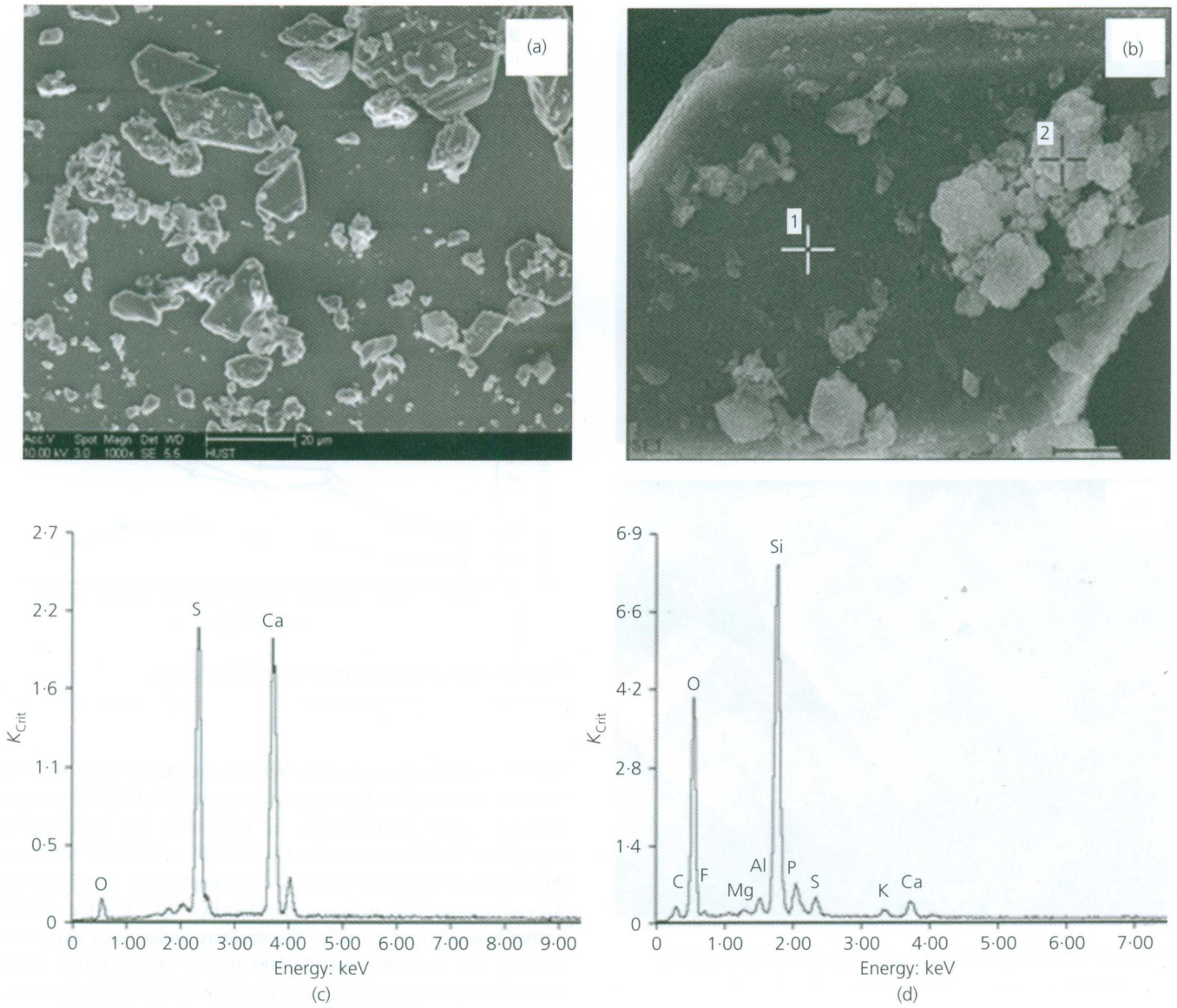

Figure 4. SEM/EDS images of original PG: (a), (b) SEM images; (c) EDS image of the first probe points; (d) EDS image of the second probe points

pentoxide and water-soluble fluoride are shown in Figure 6. It can be seen that the levels of water-soluble phosphorus pentoxide, total fluoride and water-soluble fluoride decreased significantly with an increase in calcination temperature, especially over 700°C. For sample PG-700, the water-soluble phosphorus pentoxide and water-soluble fluoride were basically below the detection limit, and the contents of total fluoride decreased from 0·34% as in the original PG to 0·11%.

The pH values of the PG samples are shown in Figure 7. The pH value increased with the increase of calcination temperature. From samples PG-0 to PG-800, the pH value increased from 4·15 to 6·64. It indicates that the water-soluble phosphorus pentoxide and water-soluble fluoride in PG decreased with the increase of calcination temperature.

Water resistance of CBPG mortars

The dry compressive strength and the wet-saturated compressive strength of CBPG mortars cured for 28 days are plotted in Figure 8. As shown, the dry and the wet-saturated strengths increased significantly with the increase in the calcination temperature. Results indicate that the maximum strength of M-700 mortar was achieved when the PG was calcined at 700°C after autoclaving. The compressive strength of CBPG mortars after WLSW or WLFW tests are also plotted in Figure 8, labelled as strength after WLSW and strength after WLFW respectively. Generally,

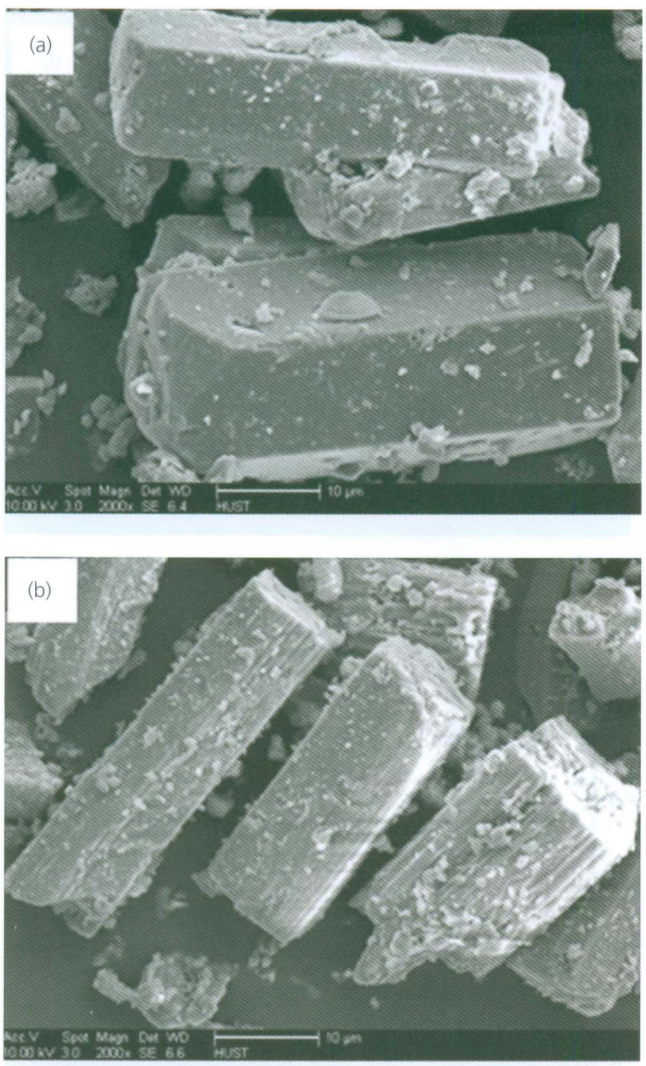

Figure 5. SEM images of pretreated PG: (a) PG-A; (b) PG-700

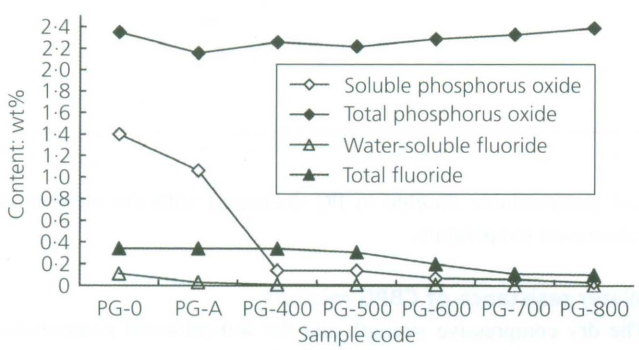

Figure 6. The content of the impurities in PG samples

both the strength after WLSW and the strength after WLFW increased with an increase of the calcination temperature. For M-0 mortar, the strength after WLFW is lower than the dry strength. However, for M-700 mortar, both the strength after

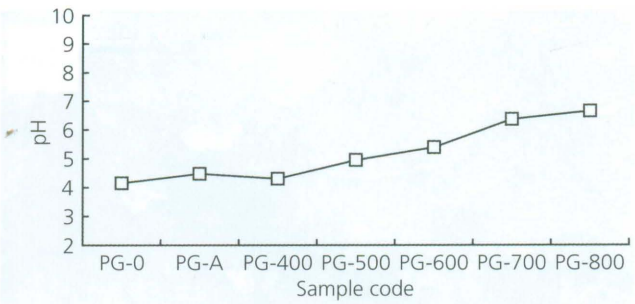

Figure 7. pH values of PG samples

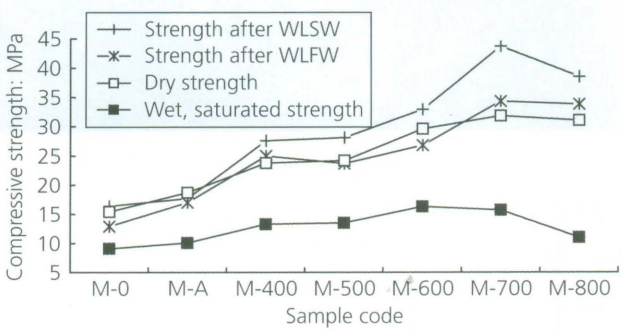

Figure 8. Compressive strength of CBPG mortars

WLSW and the strength after WLFW are higher than the dry strength. This implies that the water resistance of CBPG mortars improved after pretreatment. In particular, the compressive strength of M-700 mortar after the WLSW and WLFW tests was the highest, even higher than the dry compressive strength at 28 days of curing. This indicates that the PG–fly ash–lime system further hydrated and hardened the structure under water exposure. Overall, this indicates that M-700 mortar shows better water resistance when considering the strength of the different states, namely the dry state, wet-saturated state, after static water attack and after flowing water exposure.

The changes in WLSW and WLFW of different pretreated CBPG mortars are plotted in Figure 9. The WLSW and WLFW of different pretreated CBPG mortars decreased significantly, when compared with those of M-0 mortars. Results show that the minimum WLSW of CBPG mortars was achieved when the PG was calcined at 500–700°C after autoclaving (M-500, M-600 and M-700). The minimum WLFW of CBPG mortar, which was achieved when the PG was calcined at 700–800°C after autoclaving (M-700 and M-800), was about 0·40%. This result indicates that M-700 mortar shows better water resistance when considering WLSW and WLFW.

The traditional parameter for evaluation (W/D) of CBPG mortars is plotted in Figure 10, which shows that W/D of P-0 mortar was apparently higher than other CBPG mortars made from pretreated PG. This shows an adverse result compared with other evaluating

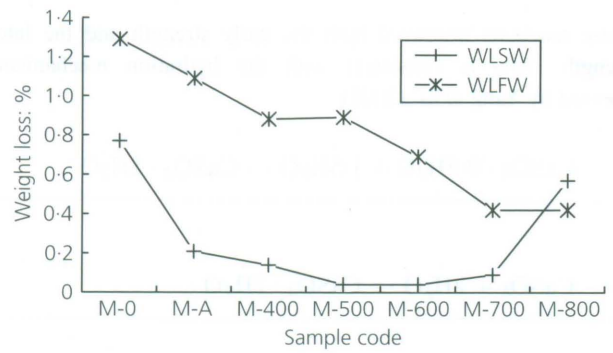

Figure 9. Weight loss of CBPG mortars after static or flowing water attack

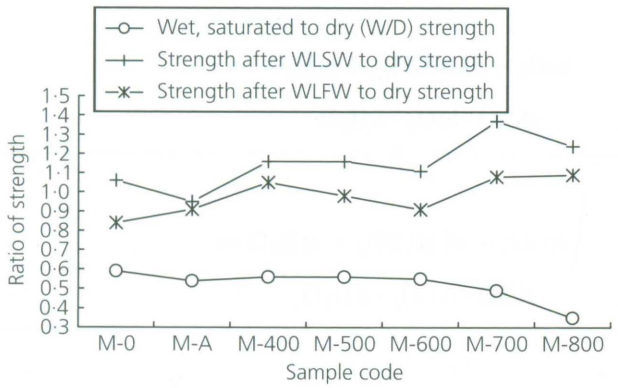

Figure 10. Ratio of compressive strength of CBPG mortars at different states to that at the dry state

parameters, namely WLSW and WLFW. Both the ratio of the compressive strength after WLSW testing to the dry strength and the ratio of the compressive strength after WLFW testing to the dry strength are plotted comparatively in Figure 10. Results indicate that both of the maximum ratios are achieved for M-700 mortar, which is consistent with the water resistance results of WLSW and WLFW testing.

Physical properties and characteristics of CBPG pastes

The physical properties of CBPG pastes are listed in Table 3. Setting time of pretreated CBPG pastes of P-A, P-400, P-500, P-600, P-700 and P-800 decreased significantly, compared with the original PG paste P-0. This was attributed to the decrease of impurities and phase transformation of gypsum after the original PG was pretreated.

The XRD patterns of P-0 paste and P-700 paste cured for different periods are shown in Figure 11 and Figure 12 respectively. Ettringite and C–S–H gel are the hydrated products that contribute to the strength of the specimens. Quartz and mullite are the main components in the unreacted fly ash, which could contribute to an increase in the long-term strength. The hydration of the new gypsum phase after pretreatment also contributed to the strength. In Figure 12, the major crystalline phase of P-700 paste cured for 28 days significantly transformed from anhydrite into dihydrate, which indicated the hydration of anhydrite during the curing days. The peaks of C–S–H in Figure 12 (P-700) are stronger than the peaks of C–S–H in Figure 11 (P-0), which is consistent with the results of the strength tests.

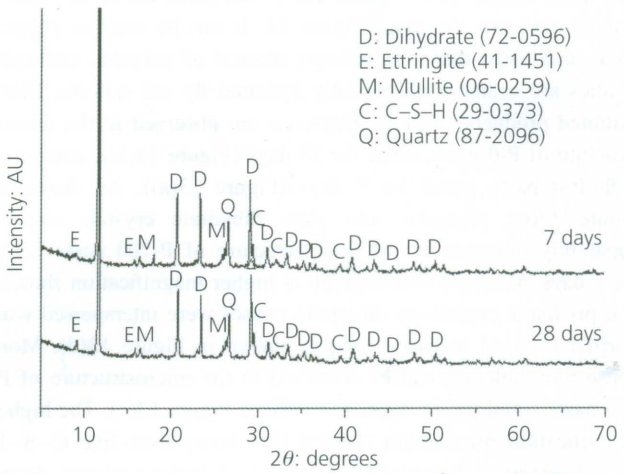

Figure 11. XRD patterns of P-0 paste specimens cured for 7 and 28 days

CBPG paste designation	Consistency	Setting time: min		Soundness
		Initial	Final	
P-0	38·0	2934	3625	Yes
P-A	34·2	1404	2040	Yes
P-400	38·5	198	389	Yes
P-500	38·0	343	548	Yes
P-600	37·5	458	684	Yes
P-700	37·0	517	705	Yes
P-800	37·5	556	746	Yes

Table 3. Physical properties of CBPG paste

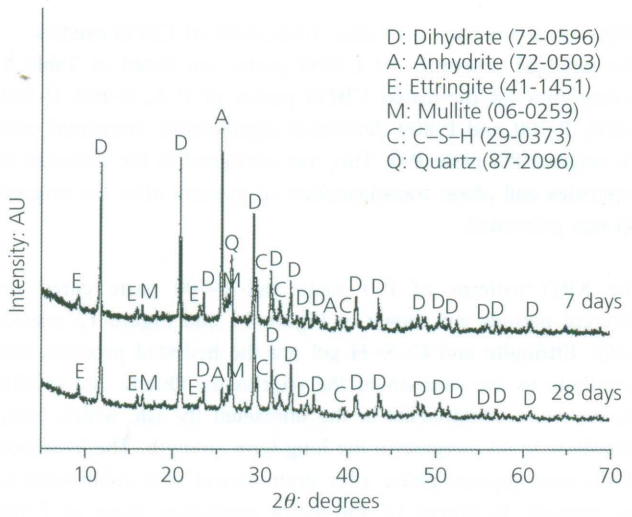

Figure 12. XRD patterns of P-700 paste specimens cured for 7 and 28 days

The SEM images of P-0 paste and P-700 paste cured for 7 days and 28 days are shown in Figure 13. It can be seen in Figures 13(a) and 13(b) that a significant amount of euhedral ettringite needles are coated with partially hydrated fly ash spheres. More hydrated products and less interspace are observed in the microstructure of P-0 paste cured for 28 days (Figure 13(b)), compared with P-0 paste cured for 7 days (Figure 13(a)). As shown in Figure 13(c), prismatic and platy dihydrate crystals can be apparently observed in the microstructure of P-700 paste cured for 7 days. Moreover, micrograph at higher magnification showed that prismatic crystals of dihydrate phases were interspersed with fibrillar C–S–H in early ages, as shown in Figure 13(d). More dense morphologies can be observed in the microstructure of P-700 paste cured for 28 days, as shown in Figure 13(e). The higher magnification micrograph showed that honeycomb-like C–S–H was observed and prismatic crystals of dihydrate phases disappeared, as shown in Figure 13(f). Morphology of P-700 paste showed denser microstructure and more C–S–H crystals in Figures 13(c)–13(f), compared with the morphology of P-0 paste in Figures 13(a) and 13(b).

The hydration process of CBPG

The XRD analysis suggests that the hydrated products are gypsum, ettringite and C–S–H gel. Dihydrate ($CaSO_4{\cdot}2H_2O$) transformed from hemihydrate (α-$CaSO_4{\cdot}0{\cdot}5H_2O$) and anhydrite ($\alpha$-$CaSO_4$), as shown in Equations 4 and 5. These reactions occurred immediately, and contributed to the early strength. The formation of C–S–H gel from $3CaO{\cdot}SiO_2$ in Portland cement is shown in Equation 6, while C–S–H gel could also be formed from silica (SiO_2) in the fly ash with lime, as shown in Equation 7. The reaction between aluminium oxide (Al_2O_3) in fly ash and lime occurred and hydration products were formed, as shown in Equation 8. Simultaneously, fly ash reacted with PG in alkaline condition and ettringite was formed, as shown in Equation 9. These reactions improved both the early strength and the later strength. This is consistent with the hydration mechanisms reported by Yang *et al.* (2008).

4. $$CaSO_4 \cdot 0{\cdot}5H_2O + 1{\cdot}5H_2O \rightarrow CaSO_4 \cdot 2H_2O$$

5. $$CaSO_4 + 2H_2O \rightarrow CaSO_4 \cdot 2H_2O$$

6. $$3CaO \cdot SiO_2 + nH_2O \rightarrow xCaO \cdot SiO_2 \cdot yH_2O + (3-x)Ca(OH)_2$$

7. $$SiO_2 + xCa(OH)_2 + mH_2O \rightarrow xCaO \cdot SiO_2 \cdot nH_2O$$

8. $$Al_2O_3 + xCa(OH)_2 + mH_2O \rightarrow xCaO \cdot Al_2O_3 \cdot nH_2O$$

9. $$6Ca^{2+} + 2AlO_2^- + 3SO_4^{2-} + 4OH^- + 29H_2O \rightarrow Ca_6Al_2(SO_4)_3(OH)_{12} \cdot 26H_2O$$

Conclusions

Phosphogypsum could be effectively purified by treating it by autoclaving and/or calcination. In particular, total fluoride, water-soluble fluoride and water-soluble phosphorus pentoxide (P_2O_5) could be reduced in these pretreated PG samples after autoclaving and then calcination at over 700°C.

The experimental results indicate that the crystalline phase of the autoclaved PG samples mostly transforms into hemihydrate (α-$CaSO_4{\cdot}0{\cdot}5H_2O$) while the crystalline phase transforms into anhydrite ($CaSO_4$) when calcined at 400–800°C for 2 h.

The test results of water resistances show that the water resistance of CBPG mortars could be improved after PG was pretreated with autoclaving and then calcination when compared with that of the original PG. The water resistance ability of CBPG mortars was best when the autoclaved PG was calcined at 700°C. Regarding the weight loss and strength after static or flowing water attack conditions, WLSW and WLFW could effectively evaluate the water resistance of CBPG mortars, compared with traditional W/D.

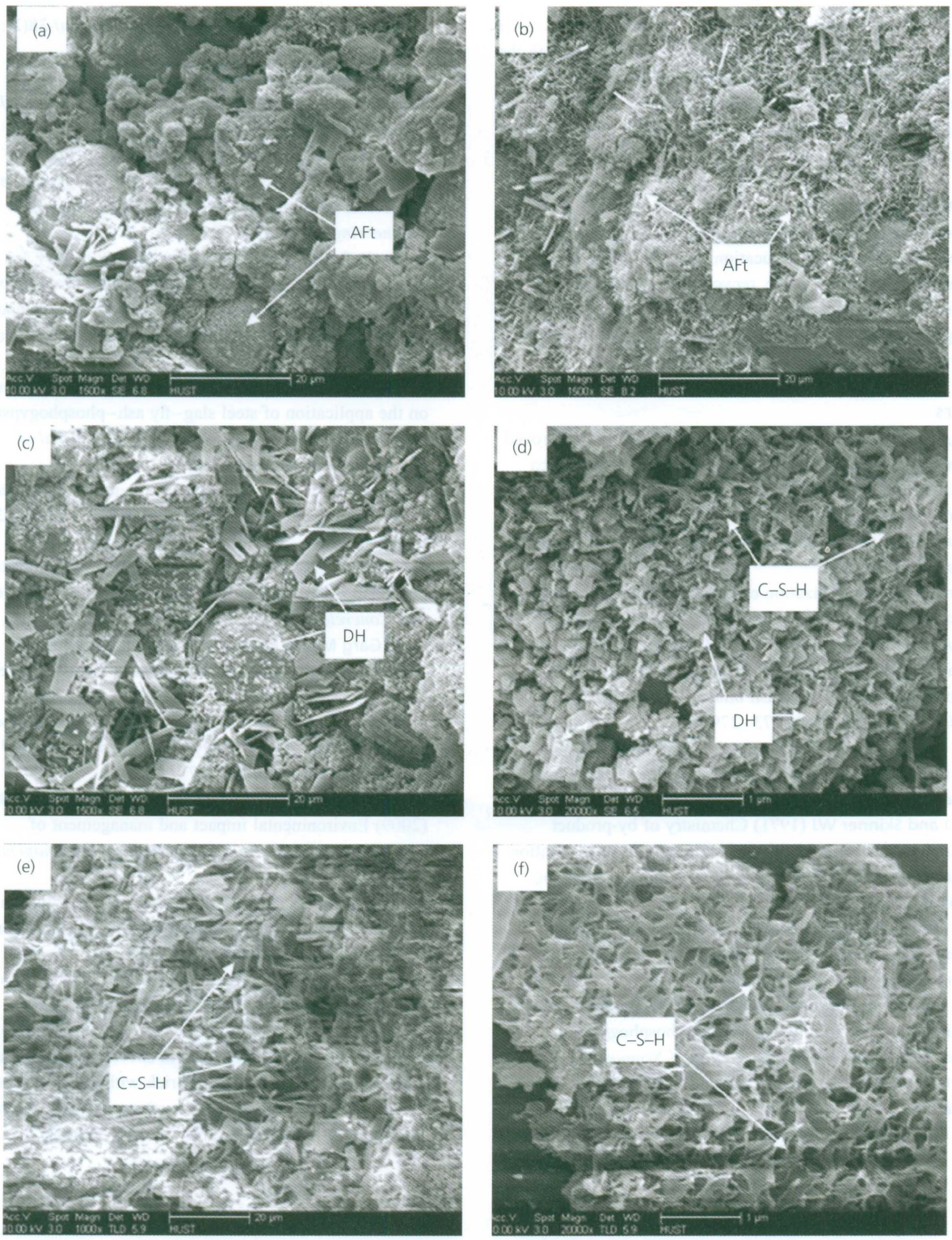

Figure 13. SEM images of paste specimens: (a) P-0 cured for 7 days with original magnification ×1500; (b) P-0 cured for 28 days with original magnification ×1500; (c) P-700 cured for 7 days with original magnification ×1500 and (d) ×20 000; and (e) P-700 cured for 28 days with original magnification ×1500 and (f) ×20 000

The XRD analysis shows that dihydrate, ettringite and C–S–H gel are the main hydration products. Dihydrate contributes to the early strength. Both ettringite and C–S–H gel contribute not only to the early strength but also to the later strength. These products coat the surfaces of fly ash and PG, and may improve the water resistance of CBPG mortars.

Acknowledgements

The authors would like to thank New Century Excellent Talents Project of the Ministry of Education (NCET-09–0392) for the funding support of solid waste recycling projects. The authors would also like to thank the Analytical and Testing Center of Huazhong University of Science and Technology for providing the experimental facilities.

REFERENCES

Bentur A, Kovler K and Goldman A (1994) Gypsum of improved performance using blends with Portland cement and silica fume. *Advance in Cement Research* **6(23)**: 109–116.

Chen Y, Yue WH and Dong RL (eds) (2003) *Gypsum Building Materials*. China Building Materials Industry Press, Beijing, China (in Chinese).

Değirmenci N (2008) Utilization of phosphogypsum as raw and calcined material in manufacturing of building products. *Construction and Building Materials* **22(8)**: 1857–1862.

Garg M and Singh M (1996) Some aspects of the durability of a phosphogypsum–lime–fly ash binder. *Construction and Building Materials* **10(4)**: 273–279.

Huang Y and Lin ZS (2010) Investigation on phosphogypsum–steel slag–granulated blast-furnace slag–limestone cement. *Construction and Building Materials* **24(7)**: 1296–1301.

Kitchen D and Skinner WJ (1971) Chemistry of by-product gypsum and plaster I. Identity of an important solid solution impurity. *Journal of Applied Chemistry and Biotechnology* **21(2)**: 53–55.

Kovler K (1998) Strength and water absorption for gypsum–cement–silica fume blends of improved performance. *Advances in Cement Research* **10(2)**: 81–92.

Kovler K and Somin M (2004) Producing environment-conscious building materials from contaminated phosphogypsum. *Proceedings of the RILEM International Symposium on Environment-conscious Materials and Systems for Sustainable Development (ECM2004), Koriyama, Japan*, 241–250.

Kumar S (2003) Fly ash–lime–phosphogypsum hollow blocks for walls and partitions. *Building and Environment* **38(2)**: 291–295.

Kuryatnyk T, Angulski LC, Ambroise J and Pera J (2008) Valorization of phosphogypsum as hydraulic binder. *Journal of Hazardous Materials* **160(2–3)**: 681–687.

Potgieter JH and Howell-Potgieter SS (2001) A plant investigation into the use of treated phosphogypsum as a set-retarder in OPC and an OPC/fly ash blend. *Minerals Engineering* **14(7)**: 791–795.

Potgieter JH, Potgieter SS and McCrindleb RI (2003) An investigation into the effect of various chemical and physical treatments of a South African phosphogypsum to render it suitable as a set retarder for cement. *Cement and Concrete Research* **33(8)**: 1223–1227.

Shen WG, Zhou MK, Ma W, Hu JQ and Cai Z (2009) Investigation on the application of steel slag–fly ash–phosphogypsum solidified material as road base material. *Journal of Hazardous Materials* **164(1)**: 99–104.

Singh M (2002) Treating waste phosphogypsum for cement and plaster manufacture. *Cement and Concrete Research* **32(7)**: 1033–1038.

Singh M (2003) Effect of phosphatic and fluoride impurities of phosphogypsum on the properties of selenite plaster. *Cement and Concrete Research* **33(9)**: 1363–1369.

Singh M, Garg M and Rehsi SS (1990) Durability of phosphogypsum based water-resistant anhydrite binder. *Cement and Concrete Research* **20(2)**: 271–276.

Singh M, Garg M and Verma CL (1996) An improved process for the purification of phosphogypsum. *Construction and Building Materials* **10(8)**: 597–600.

Tayibi H, Choura M, López FA, Alguacil FJ and López-Delgado A (2009) Environmental impact and management of phosphogypsum. *Journal of Environmental Management* **90(8)**: 2377–2386.

Yang M, Qian JS and Pang Y (2008) Activation of fly ash–lime systems using calcined phosphogypsum. *Construction and Building Materials* **22(5)**: 1004–1008.

Yang JK, Liu WC, Zhang LL and Xiao B (2009a) Preparation of load-bearing building materials from autoclaved PG. *Construction and Building Materials* **23(2)**: 687–693.

Yang JK, Xie YZ, Liu WC, Ren TY and Lin XL (2009b) Study on the preparation technology of brick with phosphogypsum pretreated by steam and its strength mechanism. *Journal of Building Materials* **12(3)**: 352–355 (in Chinese).

WHAT DO YOU THINK?

To discuss this paper, please submit up to 500 words to the editor at www.editorialmanager.com/acr by 1 June 2012. Your contribution will be forwarded to the author(s) for a reply and, if considered appropriate by the editorial panel, will be published as a discussion in a future issue of the journal.